Nano-Enhanced Electric-Field Treatment Harnessing Lightning-Rod Effect for Rapid Bacteria Inactivation

Ting Wang, Devin Brown, Xing Xie*

School of Civil and Environmental Engineering, Georgia Institute of Technology, Atlanta, Georgia 30332, United States
Institute for Electronics and Nanotechnology, Georgia Institute of Technology, Atlanta, GA 30332, United States

Abstract

The growth of undesired bacteria can cause numerous problems. Seeking effective and sustainable bacteria inactivation approaches is an everlasting effort. Here, we show that nano-enhanced electric field treatment (NEEFT) can cause rapid bacteria inactivation with a lower applied voltage than bulk EFT. A lab-on-a-chip with nanowedge-modified electrodes is developed, and the bacteria inactivation in NEEFT is visualized and studied in real-time at a single-cell level. Rapid bacteria inactivation (~ 1 ms) occurs specifically at nanowedge tips where the electric field is enhanced due to the lightning-rod effect. Nanowedges with a high aspect ratio are critical for bacteria inactivation. NEEFT works for both immobilized and free-moving cells, where the free-moving cells will be first attracted to the nanowedge tips followed by rapid inactivation. The mechanism study shows that the bacteria inactivation is caused by electroporation induced by the nano-enhanced electric field. The bacteria inactivation performance depends on the strength of the enhanced electric field instead of the applied voltage. Quick pore closure and membrane recovery under moderate NEEFT indicate that electroporation is the predominant mechanism. NEEFT only requires facile treatment to achieve bacteria inactivation, which is safe for treating delicate samples and energy-efficient for large scale applications. It is also expected to find applications for targeted cell inactivation.

Bacteria are indispensable for both ecological systems and human bodies, but the growth of undesired bacteria can also cause serious problems. Seeking approaches for bacteria inactivation is an everlasting effort. Most of our current practices for bacteria inactivation highly rely on the uses of chemicals, such as antibiotics for infection treatment, chlorine for water disinfection, antiseptics for food preservation, and chemical anti-fouling agents. They have been effectively inactivating bacteria, but caused new problems: overusing of antibiotics has already raised the concern of antibiotic resistance,[1] chlorination generates disinfection by-products (DBPs) that can be carcinogenic;[2] food antiseptics and anti-fouling agents themselves may be harmful to human health or the environment.

Effective physical processes, such as thermo/ultraviolet radiation,[3,4] acoustic vibration,[5,6] microwave,[7] and electric-field treatment (EFT),[8] can be superior alternatives to chemical approaches for bacteria inactivation, although many of them suffer from high capital cost or energy consumption. Among these processes, the EFT has been found increasing interest for food preservation and water disinfection.[9-12] The EFT aims to inactivate bacteria by electroporation: when a cell is exposed to a strong electric field, an induced transmembrane voltage (TMV) will cause pore formation on the lipid bilayer membrane,[13-15] and when this external electric field is strong enough, the membrane damage, *i.e.*, the pores, will become lethal to the bacterial cells.[10] The lethal electroporation threshold was found to be between 10 ~ 35 kV/cm.[16] Typically, in order to achieve the strong enough electric field, the EFT processes will require high applied voltages (e.g., ~ 23 kV to achieve 35 kV/cm on the electrodes with 0.65 cm distance),[17] which leads to safety issues, side reactions, and high energy consumption.

A strategy to realize the high electric-field strength with lower voltages is to decorate the electrodes with sharp objects, such as nanowires or nanowedges. Attributed to the lightning-rod effect, the electric field near the tips could be largely enhanced depending on the aspect ratio of the electrode decorations.[18] As a result, even with relatively low applied voltages, the nano-enhanced electric field can still build up the transmembrane voltage that is sufficient to cause irreversible electroporation and bacteria inactivation. Although this concept has been claimed as the predominant mechanism for bench-scale EFT water disinfection devices equipped with nanowire-modified electrodes,[19-27] direct demonstration of lightning-rod effect for bacteria inactivation, especially at the single-cell level, is not yet done. Here, we conduct nano-enhanced EFT (NEEFT) on lab-on-a-chip devices with nanowedge-modified electrodes and characterize the microbial inactivation process in-situ and in real-time. Results show that bacteria located at the tips of nanowedges on both positive and negative electrodes are rapidly inactivated at the voltages which are not sufficient to kill bacteria in bulk. Electroporation induced by the nano-enhanced electric field attributed to the lightning-rod effect is demonstrated to be the predominant mechanism for this bacteria inactivation.

Results

Visualization of bacteria inactivation by the NEEFT. We develop a lab-on-chip device with gold nanowedges fabricated on both positive and negative electrodes (**Fig. 1a** & **Fig. S1**). The gap between the two electrodes is 50 μm. The length and thickness of the nanowedge are 8 μm and 200 nm, respectively. The width of the nanowedge tip is 200 nm, and it gradually increases to 1 μm to allow a steadier connection to the bulk electrode. This is the default chip design for our experiments unless otherwise stated. When an 18 V voltage is applied to the two electrodes, the

electric field near the nanowedge tips will be enhanced due to the lightning-rod effect, which is simulated using COMSOL Multiphysics (**Fig. 1b**).

Model bacteria *Staphylococcus epidermidis* (*S. epidermidis*) cells immobilized on the poly-L-lysine coated chip are uniformly distributed between the positive and negative electrodes (**Fig. 1c**). Live-and-dead cell distinguishing stain propidium iodide (PI) was added in the deionized water (DI water) medium before treatment (See experimental setup in **Fig. S2a**). After 500,000 electrical pulses at 18 V with 2 µs pulse width and 100 µs period are applied (denoted as 18 V/2 µs/100 µs/500,000 pulses, see the waveform in **Fig. S3**), the bacteria at the tips of nanowedges on both positive and negative electrodes show red fluorescence of the PI stain, indicating cell inactivation, while cells anywhere else are intact (**Fig. 1d**). The zoom-in image clearly shows that only the cells located very close to the nanowedge tips are inactivated, which is consistent with the electric field enhancement pattern **(Fig. 1b)**. By comparison, for the electrodes that have no nanowedge modification but a smaller gap of 34 µm, hardly any cells are inactivated (**Fig. S4**), suggesting that this treatment is not sufficient to kill bacteria in bulk. Therefore, NEEFT can cause bacteria inactivation with lower applied voltages than in bulk-EFT. To the best of our knowledge, this is also the first time that the bacteria inactivation in NEEFT is visualized at the single-cell level.

The bacteria inactivation process is observed in real-time. The onset position of PI fluorescence indicates that the cell membrane damage takes place at the position adjacent to the nanowedge tip, where the nano-enhanced electric field has the highest strength. The circled bacteria cells are at the nanowedge tips on the negative electrode (**Fig. 1e**) and positive electrode (**Fig. 1f**), and they do not show fluorescence before the treatment (0 s). The arrows indicate the location where the cell membrane is adjacent to the nanowedge tip. After the treatment starts, the red fluorescence of PI stain first originates from the position where the cell is adjacent to the nanowedge tip as indicated by the arrows (shown in 0.1 s, 0.2 s, and 0.4 s), suggesting that the part of the cell membrane subjected to the strongest electric field will be perforated first.

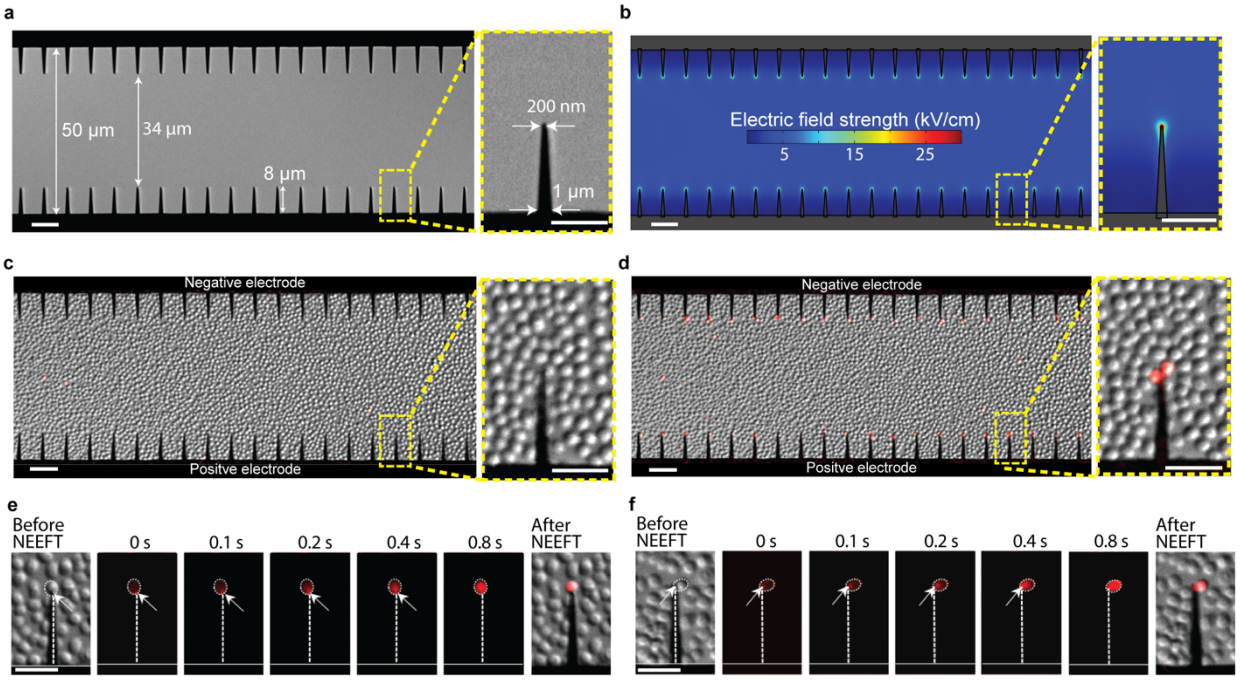

Figure 1. Bacteria inactivation in NEEFT. (a) Microscopy image of the lab-on-a-chip device. (b) Nano-enhanced electric field at the nanowedge tips at 18 V applied voltage. (c & d) Microscopy images of the immobilized bacteria cells before (c) and after (d) NEEFT treatment. Scale bars are 10 µm in normal images and

5 μm in the zoom-in images. (e & f) PI fluorescence onset indicating pore formation position of a cell at nanowedge tip on negative electrode (e) and positive electrode (f). The arrows indicate the position of the cell membrane adjacent to the nanowedge tip, which is also the onset position of PI fluorescence. Scale bars are 5 μm.

The observed bacteria inactivation process also shows that bacteria inactivation in NEEFT is very quick (**Video S1**). To figure out how fast this inactivation occurs, different effective treatment time (i.e., the total time that the applied voltage is not zero, equals to pulse width × pulse number) is tested by applying different pulse numbers of 2 μs/100 μs pulses. Under 30 V and 18 V applied voltage, 0.1 ms and 1 ms of effective treatment times are long enough to achieve >80% bacteria inactivation (represented as the percentage of nanowedges inducing bacteria inactivation at tips), indicating that bacteria inactivation in NEEFT is a very rapid process (**Fig. 2a**). Under relatively lower applied voltages (14 V and 10 V), bacteria inactivation stays at low percentages up to 1000 ms of effective treatment time, suggesting that the limiting factor of the lower bacteria inactivation is the applied voltage rather than treatment time (**Fig. 2a**). Therefore, the bacteria inactivation at different applied voltages with 1000 ms effective treatment time are tested. The bacteria inactivation shows a positive correlation with the applied voltage (**Fig. 2b**). The inactivation starts at a low voltage of 10 V, and 20 V is already high enough to achieve bacteria inactivation for almost all nanowedges, and there is no significant difference between the positive and negative electrodes. The high aspect ratio of the nanowedges is important to the NEEFT, indicated by the control experiments with different chip designs (**Figs. 2c - f**). After EFT of 18 V/2 μs/100 μs/500,000 pulses, the nanowedges with 200 nm width at the tip (**Figs. 2c & e**) and 8 μm length (**Figs. 2d & f**) show a much higher percentage of bacteria inactivation than other wider or shorter electrode modifications.

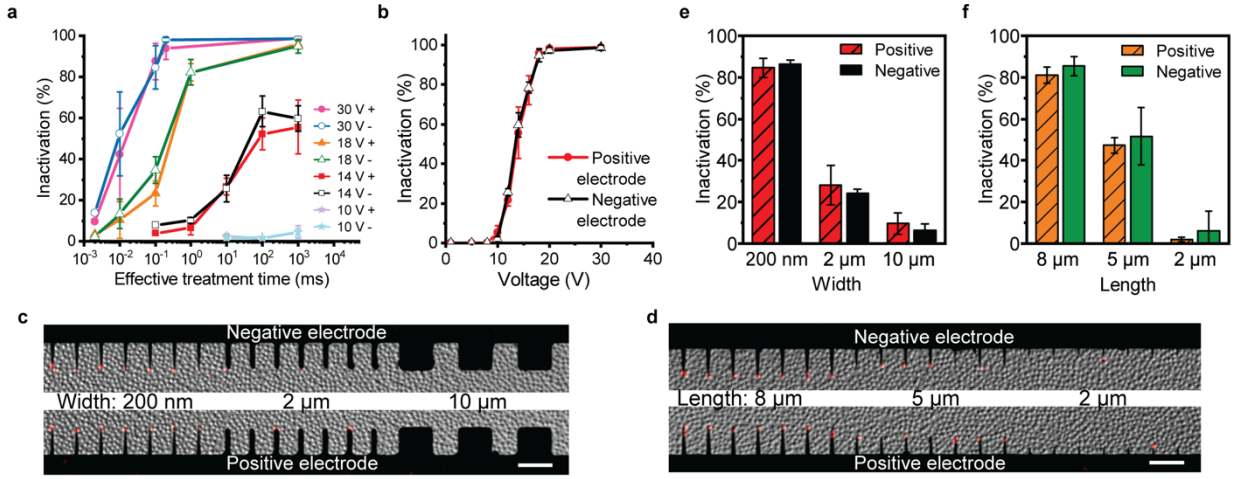

Figure 2. Bacteria inactivation characterization in NEEFT. (a) Bacteria inactivation (i.e., the percentage of nanowedges inducing bacteria inactivation) with different effective treatment time. Positive and negative electrodes are denoted as + and −, respectively. (b) Bacteria inactivation versus the applied voltage with 1 s effective treatment time. (c - f) Bacteria inactivation with wedges of different width (c & e) and different length (d & f). The scale bars are 10 μm.

NEEFT also works for free-moving bacteria cells suspended in the medium. Syto 9 and PI stained *S. epidermidis* are suspended in DI water before the treatment (**Fig. 3a upper**. See the experimental setup in **Fig. S2b**). During the NEEFT (18 V/2 μs /100 μs/500,000 pulses), bacteria cells are attracted toward the nanowedges on both positive and negative electrodes, especially to the tips. Subsequently, those near the tips get inactivated, indicated by switching from green

fluorescence of Syto 9 to red fluorescence of PI (**Video S2**, **Fig. 3a lower**). As the bacteria cells are negatively charged in DI water, most of them accumulated at the positive electrode because of the electrophoretic force. Some cells are attracted to the nanowedge tips on the negative electrode, which is probably due to the strong dielectrophoretic force induced by the electric-field enhancement near the tips.[28,29] Two other kinds of bacteria, *Bacillus subtilis* (*B. subtilis*, Gram +) and *Escherichia coli* (*E. coli*, Gram −), are also tested, which show similar transport and inactivation phenomena with *S. epidermidis* (**Figs. 3b & c**, **Videos S3 & S4**), suggesting that NEEFT could be a wide spectrum bacteria inactivation method.

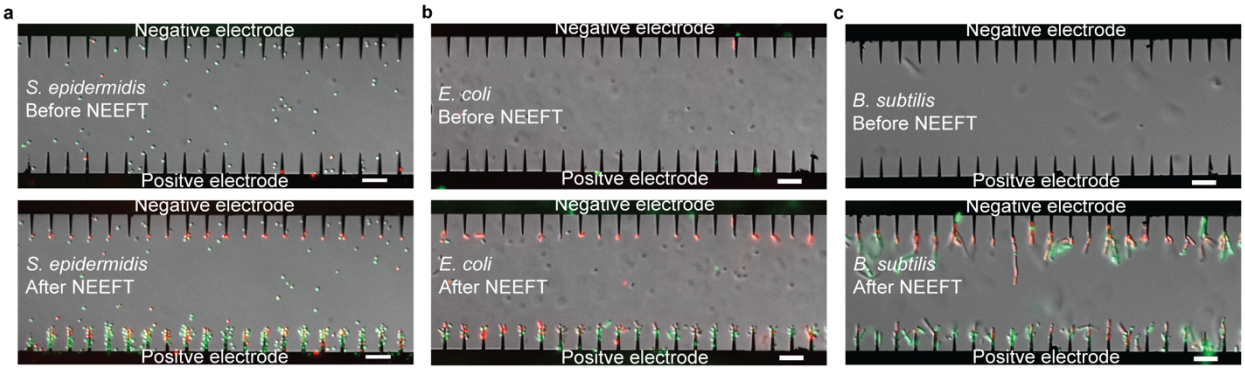

Figure 3. Microscopy images of different kinds of bacteria in suspension before (upper) and after (lower) the NEEFT. (a) *S. epidermidis*. (b) *E. coli*. (c) *B. subtilis*. The scale bars are 10 μm.

Mechanism of bacteria inactivation in nano-enhanced EFT.

In NEEFT, only the bacteria located near nanowedge tips are inactivated, while bacteria in bulk are not affected. This pattern is consistent with the electric field enhancement of nanowedges due to the lightning-rod effect. Therefore, irreversible electroporation induced by the enhanced electric field is considered as the predominant mechanism for bacteria inactivation in NEEFT. Here, we investigate this mechanism and the evidence collected is discussed below. In these studies, model bacteria *S. epidermidis* are all immobilized on the chip for more precise characterization.

The bacteria inactivation depends on the strength of the nano-enhanced electric field.

To verify whether the observed bacteria inactivation is directly due to the nano-enhanced electric field instead of the applied voltage, chips of different positive/negative electrode gaps (25 μm, 50 μm, 100 μm) and with nanowedges of different intervals (0.8 μm, 4 μm, 40 μm) are tested for bacteria inactivation. The strength of the nano-enhanced electric field is reversely proportional to the gap between the two electrodes (**Figs. S5a & b**). Therefore, with the same applied voltage, chips with a smaller gap achieve a higher percentage of bacteria inactivation (**Fig. 4a & Fig. S5c**). Similarly, because of the stronger lightning-rod effect for electric-field enhancement (**Figs. S6a & b**), the nanowedges with a larger interval in between could achieve higher bacteria inactivation under the same applied voltage (**Fig. 4b & Fig. S6c**). When all the results are analyzed, the percentage of bacteria inactivation at the tips of nanowedges shows a positive correlation with the electric field strength (**Fig. 4c left**), but not with the applied voltage (**Fig. 4c right**). This result indicates that the bacteria inactivation is attributed to the nano-enhanced electric field.

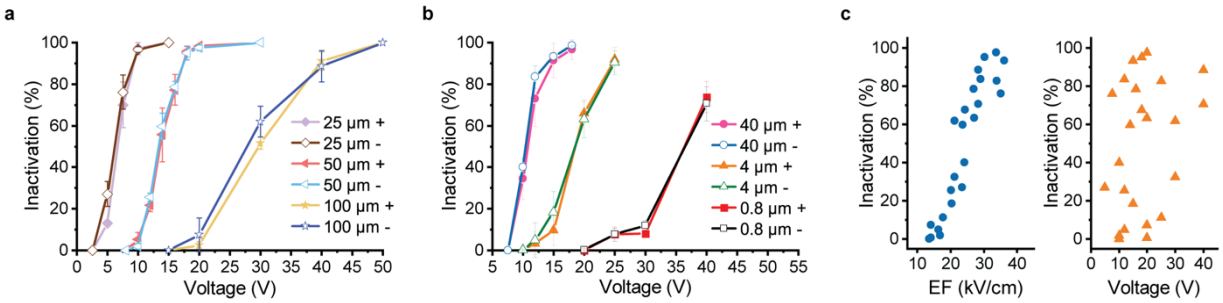

Figure 4. Bacteria inactivation with different chip designs. (a) Bacteria inactivation on chips of different gaps between positive and negative electrodes. (b) Bacteria inactivation on chips of different intervals between nanowedges. (c) Relationship between the bacteria inactivation and the electric field strength (EF) at the tip of the nanowedge (0.1 μm away from the nanowedge tip) (left), and the applied voltage (right).

The bacteria inactivation is not attributed to reactive oxygen species (ROS).

Electric-field treatment systems could generate ROS, especially under high voltages or long treatment times. To test if the bacteria inactivation is attributed to ROS damage, DCFH-DA stain is used to detect ROS generation.[30,31] In the experiment group with 30 V/2 μs/100 μs/100,000 pulses treatment, DCFH-DA stained cells show no fluorescence (**Fig. 5a**), suggesting no ROS generation. Meanwhile, >90% bacteria inactivation is achieved (**Fig. 5b & experiment group, no DMSO in Fig. 5g**), indicating that this bacteria inactivation is not due to ROS damage. To confirm this ROS detection method is valid, we intentionally induce ROS generation with a much longer pulse width in the positive control (20 V/200 μs/10 ms/1000 pulses). The significant green fluorescence of DCFH-DA stained cells shows that ROS is generated near the positive electrode (**Fig. 5d**). The positive electrode shows more inactivated bacteria at each nanowedge tip than the experiment group and negative electrodes (**Fig. 5e & positive control, no DMSO in Fig. 5g**), which could be attributed to the ROS damage.

To further confirm that the bacteria inactivation at 30 V/2 μs/100 μs is not due to ROS generation, a ROS scavenger, DMSO, is added to the medium at 15% (w/w) to quench ROS and protect bacteria from ROS damage.[32] In the positive control group, the bacteria at the positive electrodes are largely protected by DMSO (**Fig. 5f & positive control in Fig. 5g**), proving that 15% DMSO is able to protect bacteria from ROS damage. In the experiment group, even with the ROS scavenger DMSO, the bacteria inactivation percentage and inactivated cell number are not affected (**Fig. 5c & experiment group in Fig. 5g**), which further confirms that the bacteria inactivation is not due to ROS damage.

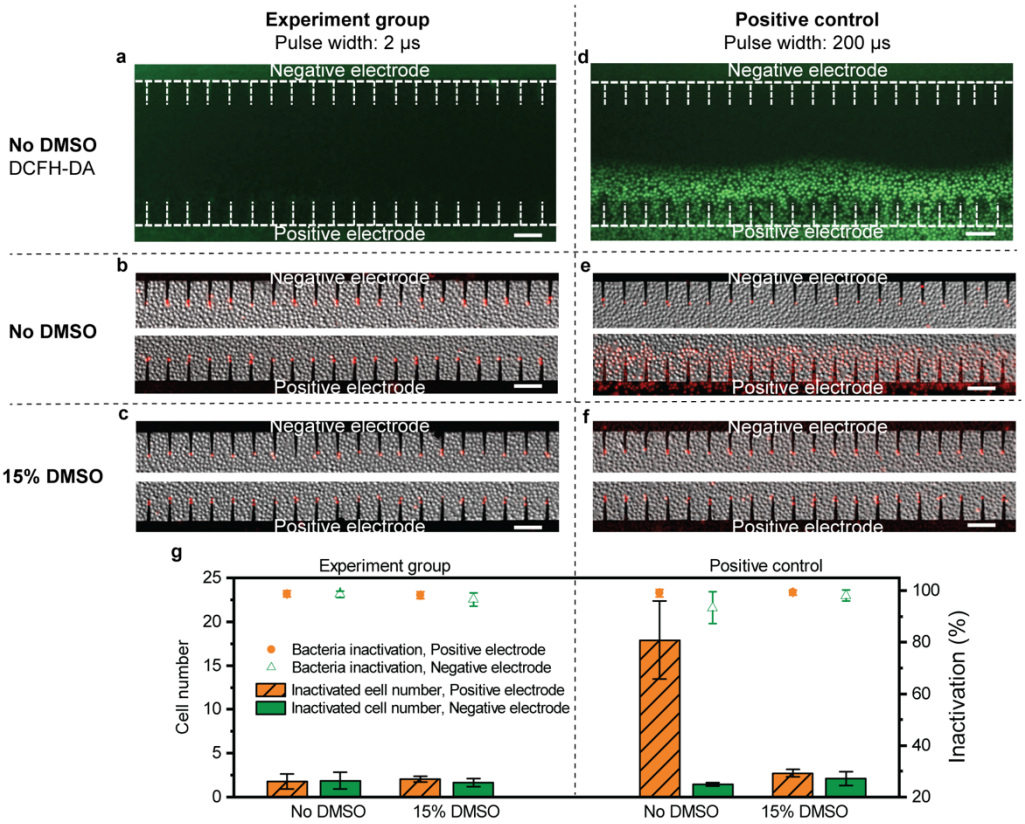

Figure 5. Detection of ROS generation. (a) Fluorescence of DCFH-DA stained cells in experiment group. (b & c) Bacteria inactivation in experiment group with no DMSO (b) and with 15% DMSO (c). (d) Fluorescence of DCFH-DA stained cells in positive control group. Green fluorescence indicates ROS generation. (e & f) Bacteria inactivation in positive control without DMSO (e) and with 15% DMSO (f). (g) Bacteria inactivation percentage and average inactivated cell number at each nanowedge tip. Scale bars are 10 μm.

Quick cell membrane recovery supports electroporation as the main bacteria inactivation mechanism.

Reversible electroporation is a phenomenon that pores formed on the lipid bilayer membrane will reseal automatically after the electric field is removed. It occurs when the cell is exposed to a relatively weaker electric field than irreversible electroporation.[10] The PI fluorescence intensity of four cells under 14 V/2 μs/100 μs intermittent treatment shows that when the treatment is on (red zoon, 1 s), the fluorescence increases, which means pore formation and PI dye inflow (**Fig. 6a**). When the treatment is removed (gray zoon, 5 s), the fluorescence stops rising immediately, suggesting that the pores close and the membrane regains its integrity after the treatment stops (**Fig. 6a**). This kind of quick cell membrane recovery is a common phenomenon in reversible electroporation,[13,14] but is hard to find in other kinds of membrane damages, such as direct oxidation. Therefore, quick pore reseal is strong evidence for reversible electroporation.

Reversible electroporation is also tested using a double staining method with SYTOX Green and PI, which are both cell impermeable stains that can only enter cells with compromised membrane.[33] SYTOX Green is first added to the medium (Time point 1, **Fig. 6b**). After the NEEFT is applied, perforated cells are stained with SYTOX Green and show green fluorescence (Time point 2, **Fig. 6b**). After 10 minutes, PI is added, which could only stain the cells that still have compromised membrane. Thus, the cells that are not stained with PI are considered as having reversible pores (Time point 3, **Fig. 6b**). With a relatively low applied voltage at 14 V (2 μs/100

μs/20,000 pulses), some already perforated cells could not then be stained with PI, indicating the pores formed on the cell membrane are reversible (**Fig. 6c**). While under a high applied voltage at 80 V (1 μs/1 ms/10 pulses), almost all cell perforation is irreversible, since cells stained with SYTOX Green are also stained with PI (**Fig. S7**). This phenomenon conforms to the feature of electroporation, indicating that electroporation is the predominant mechanism for bacteria inactivation in NEEFT.

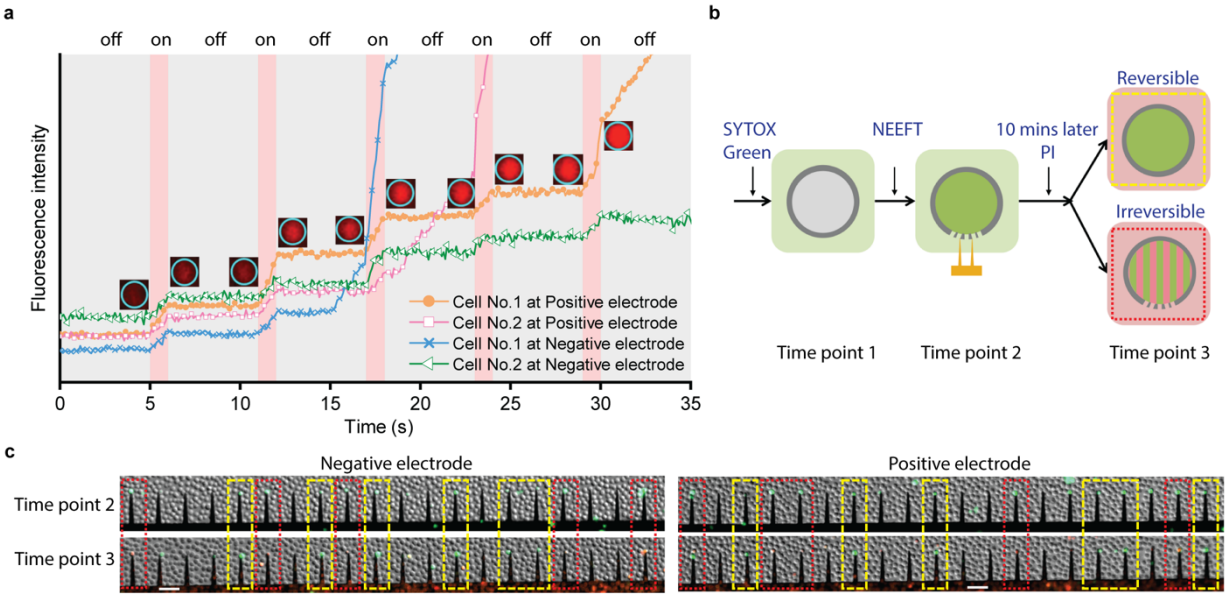

Figure 6. Detection of reversible electroporation. (a) Increase of PI stain fluorescence of four cells at nanowedge tips on positive and negative electrodes, respectively, with intermittent NEEFT. The pink zoon indicates that the NEEFT is on, which are 14 V/2 μs/100 μs/10,000 pulses for 1 s. The gray zoon indicates that the NEEFT is off, which is 0 V for 5 s. The inserted images show Cell No. 1 at the positive electrode (orange spheres). (b) Schematic of double staining method with SYTOX Green and PI for reversible electroporation detection. (c) Microscopy images showing reversible electroporation under 14 V. The cells inside the yellow frames had reversible pores on membrane since they are stained with SYTOX Green at Time point 2 but are not stained with PI at Time point 3. The cells inside the red frames have irreversible pores since they are first stained with SYTOX Green and then stained with PI. Scale bars are 5 μm.

Discussion on mechanisms

In this work, we for the first time show the bacteria inactivation by NEEFT at the single-cell level and demonstrate the mechanism to be electroporation induced by the lightning-rod effect of the nanowedges. Due to the lightning-rod effect, the electric field at the tips of metal rods with a high aspect ratio will be greatly enhanced compared to that in bulk. Therefore, this strong electric field could be sufficient to charge cell membrane, cause irreversible electroporation, and kill bacteria even under lower applied voltages.

Although bench-scale NEEFT for water disinfection was developed based on this concept, the mechanism was only supported by control experiments done with electrodes with/without nanowire modifications.[19,23] There was no direct evidence confirming that the bacteria were inactivated due to the nano-enhanced electric field and electroporation. The results achieved in this study provide important evidence on the mechanisms. Firstly, only the bacteria in the area of the nano-enhanced electric field are inactivated while others in bulk are intact (**Fig. 1b & d**). The inactivation percentage shows a positive correlation with the strength of the nano-enhanced electric field instead of the applied voltage (**Fig. 4**). Furthermore, when >90% bacteria inactivation

is achieved with NEEFT at 30 V/2 μs/100 μs, there is no significant ROS generation (**Fig. 5a)**, indicating this bacteria inactivation is not due to ROS damage. Reversible electroporation is detected under relatively low applied voltage (**Fig. 6**), indicating that NEEFT could induce electroporation, and irreversible electroporation causing bacteria inactivation will be dominant at higher voltages. The rapidness of the cell damage (< 1 ms) also conforms with the property of electroporation (**Fig. 2a**).

It is worth noticing that electric field enhancement by nanowedges is the same for both positive and negative electrodes (**Fig. S5 & S6**). Consistently, all the bacteria inactivation phenomena discussed above do not show a significant difference between positive and negative electrodes. In an electrochemical disinfection study, significantly higher bacteria inactivation efficiency on the anode was found compared to the cathode, suggesting that electrical reduction should not cause the same level of cell damage as electrical oxidation.[34] Our positive control group for ROS detection also confirms that (**Fig. 5e**). Therefore, the same phenomenon on both electrodes found in this work indicates that electrical oxidation/reduction should not be the mechanism causing bacteria inactivation. Therefore, electroporation is demonstrated as the predominant mechanism causing bacteria inactivation in NEEFT.

Theoretical analysis: NEEFT versus Bulk EFT

Since electroporation is the predominant mechanism for bacteria inactivation in NEEFT, the induced transmembrane voltage (TMV), which is the increased potential difference across the cell membrane resulting from exposure to an external electric field, is analyzed theoretically using finite element method to compare NEEFT and bulk EFT. Both the on-chip system like the one used in this work (**Fig. 7**) and a 3D system with standing nanowire (**Fig. S8**) are simulated. Two cells in NEEFT and bulk EFT respectively are compared, which is cell No. 1 located at the nanowedge tip (**Fig. 7a left**), and cell No. 2 located between two electrodes without nanowedge (**Fig. 7a right)**. Two concentric spheres are built to represent the inner and outer surface of the bacteria cell wall.[35] The diameter of the cell is 1 μm and cell wall thickness is 50 nm.[36] The simulation results show that the voltage drop across the membrane, i.e., the electric field, is greatly enhanced at cell No. 1 near the nanowedge tip (**Fig. 7b left**) compared to cell No. 2 (**Fig. 7b right**). The maximum TMVs of the two cells show that with the same applied voltage, the cell No. 1 in NEEFT located at the nanowire tip can achieve around 7.5 times higher TMV than cell No. 2 in bulk EFT (**Fig. 7c**), indicating that much lower voltage could be applied to achieve the same level of TMV on cells in NEEFT than bulk EFT.

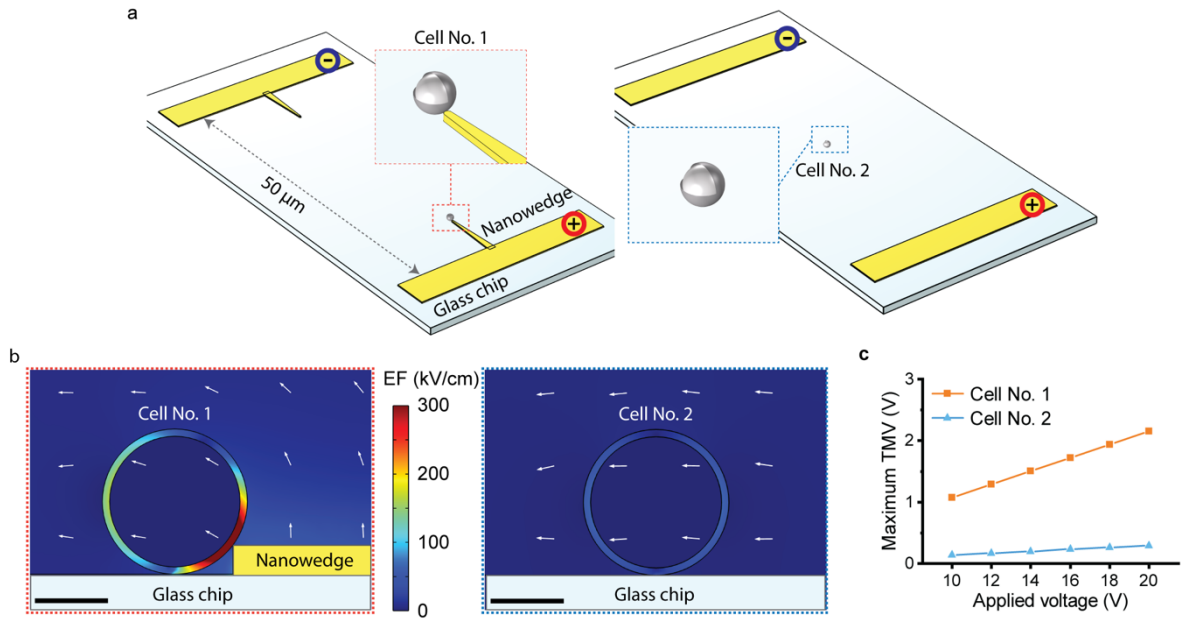

Figure 7. Theoretical analysis of cell TMV in NEEFT and bulk EFT. (a) Simulation set up for NEEFT (left) and bulk EFT (right). (b) Left view of the middle cutting plane showing the electric field across the cell membrane of cell No. 1 in NEEFT (left) and cell No. 2 in bulk EFT under 20 V applied voltage (right). The arrows indicate the direction of the electric field. The scale bars are 0.5 μm. (c) Maximum TMV on cell No. 1 and cell No. 2 under different applied voltages.

Potential applications and future studies of NEEFT

NEEFT effectively kill bacteria with mild treatment conditions without causing electrochemical reactions or other side effects, making it suitable for high-quality sample processing, such as liquid food or blood sample. The mild treatment conditions also make it a safe process, which is expected to find medical applications, such as for wound healing. Furthermore, it is an energy-efficient approach that is applicable for large-scale treatment processes, such as drinking water treatment. Since it is a highly localized bacteria inactivation process, it is perfect for biofilm control, which has potential applications in biofouling prevention. On the other hand, although NEEFT is not a homogeneous process, we have shown that in a dynamic system, bacteria could be attracted to the nanowedge tips where they then get inactivated. This targeted cell transportation occurred in NEEFT makes it possible for broad applications in continuous flow systems. The as-shown rapid cell damage and the effectiveness of both electrodes further improve its efficiency. Last but not least, NEEFT should also work on other kinds of cells in addition to bacteria since electroporation targets the lipid bilayer membrane. Therefore, it has much broader potential applications, including intracellular molecule delivery and cell lysing for a broad range of cell types.

To enhance the applications of NEEFT in dynamic systems treating free-moving cells, it is critical to transport the targeted cells to the effective zone, which is the tips of nanowedges or nanowires. Therefore, a future study is to investigate cell transportation in NEEFT system, including using electrical pulses with different parameters to control cell transport, using devices or reactors with specific designs to increase the transport of targeted cells to the effective zoon, or introducing baffles or increasing flow mixing to increase the probability of transporting cells to the effective zoon.

Methods

Chip fabrication and pre-treatment

Glass wafer was used as the substrate for electrode deposition. Gold nanowedges were first defined by electron beam lithography. Then, 200 nm gold layer was deposited using electron beam evaporation and lift-off method. The gold bulk contact pads of 300 nm thickness were defined by photolithography and fabricated by lift-off method (**Figure S1**). There are 330 nanowedges on one chip in total. The interval between nanowedges are 7 μm, which is to deploy a large number of nanowedges without interference between each other on showing bacteria inactivation phenomenon. The default nanowedge is 200 nm wide at the tip and 1 μm wide at the base in default chips. Note that the chips designed for interval experiments (Fig. 4b and S6) have nanowedges of 200 nm width tip and 400 nm width base in order to achieve 800 nm interval. To achieve bacteria immobilization on the chip, the chip was first washed and coated with poly-L-lysine (0.01%, mw 150,000-300,000). The detailed methods are stated in supplementary information.

Cell culture and harvest

S. epidermidis or B. subtilis were cultured in nutrient broth for 15 hours, and *E. coli* was cultured in LB broth for 7 hours before use. For the immobilized cells, 4 mL bacterial solution was centrifuged at 4000 rpm for 5 min. The supernatant was discarded, and the bacterial pallet was resuspended in 1 mL 10 mM phosphate buffer. After 3 times of washing, the cell pallet was resuspended in 0.5 mL 10 mM phosphate buffer to achieve the bacteria suspension with a higher cell concentration. For the experiment with free-moving cells, bacteria were washed with DI water for 3 times instead of phosphate buffer.

Experimental setup for immobilized bacteria cells

To conduct NEEFT with immobilized bacteria cells, add 40 μl of prepared bacteria suspension onto a poly-L-lysine coated chip to cover the gap between two electrodes, then let the cells settle down for 50 mins in room temperature. During this time, a layer of cells will be immobilized on the chip surface. Then, the bacterial solution on the chip was gently washed away with 4 ml DI water containing 15 μM Propidium iodide (PI) using a pipette, to remove the non-immobilized cells and leave the immobilized bacteria in a drop of PI staining DI water. The chip was then flipped, put onto a coverslip, loaded onto an inverted microscope for *in situ* observation (see experimental setup in **Fig. S2**).

Experimental setup for free-moving bacteria cells

To visualize the bacteria inactivation process with free-moving bacteria, stain bacteria in the prepared bacteria suspension with 15 μM PI and 5 μM SYTO 9 (Thermo Fisher Scientific) for 5 min before use. Add 40 μl of stained bacteria suspension onto the chip to cover the gap between two electrodes. Then the chip was flipped, put onto a coverslip, and loaded onto an inverted microscope for *in situ* observation (see experimental setup in **Fig. S2**).

NEEFT procedures

The pulsed voltages were applied to the chip using a pulse generator (Avtech Electrosystems LTd.) which is triggered with a waveform generator (Keysight 33509B). The typical pulses used in this work have 2 μs pulse width, 100 μs period (10 kHz), 500,000 pulses, corresponding to 1 s effective treatment time and 50 s total time, unless stated otherwise. The effective treatment time is the total time when the applied voltage is not 0, which equals pulse width × pulse number. The

pulse width of 2 μs is used to minimize electrochemical reactions. The pulse waveform was measured using an oscilloscope (Keysight InfiniiVision 6000 X-series).

ROS detection

For ROS detection experiments, the ROS indicator DCFH-DA was added to stain the bacteria at 0.2 mM during the bacteria immobilizing process for 50 min. After staining, DCFH-DA was washed away with DI water. To ensure that this method is able to detect ROS generation, pulses with longer pulse width (200 μs/10 ms) at 20 V were tested as positive control. Significant fluorescence near the positive electrode was observed, indicating this method is valid for ROS detection.

In DMSO test, DI water containing 15% DMSO and 15 μM PI was used as the medium to quench ROS and protect bacteria form ROS damage.

Reversible electroporation tests

For reversible electroporation tests, 5 μM SYTOX Green was first added to the medium before treatment. Electrical pulses of 14 V/2 μs/100 μs/20,000 pulses were applied, and the microscopy images were collected. Ten minutes after the electrical treatment, 15 μM PI was then added, and the images were collected again.

Microscope observation

The NEEFT treatment process was observed and recorded *in situ* using an inverted fluorescence microscope (Zeiss Axio Observer 7). Cell and nanowedge images were captured via DIC channel. PI was excited at 488 nm. Syto 9, and SYTOX Green, and DCFH-DA were excited at 555 nm, respectively. In supporting video 2, 3 and 4, the electrode and nanowedges are visualized using reflection channel with 555 nm incident light. All fluorescent signals are filtered with a 90 HS filter. The video taking was triggered by the Keysight 33509B waveform generator.

Image processing and data statistics

The microscopy images were processed using MATLAB. The fluorescence image of PI signal before treatment was subtracted from the image after treatment, which only keeps the changing of PI signal. The subtracted image was then processed for inactivation and counting analyzing.

The bacteria inactivation percentage is represented as the percentage of nanowedges that have inactivated cell at the tip, which is

$$Bacteria\ inactivation\ (\%) = \frac{number\ of\ nanowedges\ that\ have\ dead\ bacteria\ at\ tip}{total\ number\ of\ nanowedges}.$$

There are 330 nanowedges on one chip for the default design. Each treatment experiment was repeated with three chips, and the error bars show the standard deviation of the three repeated experiments. Note that for the chips that have 0.8 um interval nanowedges, cell number at the nanowedge tip is less than nanowedge number due to the small interval. Bacteria inactivation is represented as the percentage of dead cells, which is

$$Bacteria\ inactivation\ (\%) = \frac{number\ of\ dead\ bacteria\ at\ nanowedge\ tips}{total\ number\ of\ bacteria\ at\ nanowedge\ tips}.$$

Electric field and TMV simulation

The nano-enhanced electric field and transmembrane voltage (TMV) was simulated using electric current module in COMSOL Multiphysics. The detailed methods are stated in supplementary information.

Declaration of Competing Interest

The authors declare no competing financial interest.

Acknowledgements

The authors acknowledge the financial support from the National Science Foundation [grant numbers CBET 1845354]. This work was performed in part at the Georgia Tech Institute for Electronics and Nanotechnology, a member of the National Nanotechnology Coordinated Infrastructure (NNCI), which is supported by the National Science Foundation [grant numbers ECCS-1542174]. T.W. is grateful for the financial support provided by the China Scholarship Council.

REFERENCES

1 Neu, H. C. The crisis in antibiotic resistance. *Science* **257**, 1064-1073 (1992).

2 Sedlak, D. L. & von Gunten, U. The chlorine dilemma. *Science* **331**, 42-43 (2011).

3 McKinney, C. W. & Pruden, A. Ultraviolet disinfection of antibiotic resistant bacteria and their antibiotic resistance genes in water and wastewater. *Environmental science & technology* **46**, 13393-13400 (2012).

4 Hijnen, W. A. M., Beerendonk, E. F. & Medema, G. J. Inactivation credit of UV radiation for viruses, bacteria and protozoan (oo)cysts in water: A review. *Water Research* **40**, 3-22, doi:10.1016/j.watres.2005.10.030 (2006).

5 Gao, S., Hemar, Y., Ashokkumar, M., Paturel, S. & Lewis, G. D. Inactivation of bacteria and yeast using high-frequency ultrasound treatment. *Water research* **60**, 93-104 (2014).

6 Lu, H. *et al.* Rapid additive-free bacteria lysis using traveling surface acoustic waves in microfluidic channels. *Lab on a Chip* **19**, 4064-4070 (2019).

7 Plazas-Tuttle, J., Das, D., Sabaraya, I. V. & Saleh, N. B. Harnessing the power of microwaves for inactivating Pseudomonas aeruginosa with nanohybrids. *Environmental Science: Nano* **5**, 72-82 (2018).

8 Grahl, T. & Markl, H. Killing of microorganisms by pulsed electric fields. *Applied Microbiology and Biotechnology* **45**, 148-157, doi:10.1007/s002530050663 (1996).

9 Barba, F. J. *et al.* Current applications and new opportunities for the use of pulsed electric fields in food science and industry. *Food Research International* **77**, 773-798 (2015).

10 Kotnik, T. *et al.* Electroporation-based applications in biotechnology. *Trends in biotechnology* **33**, 480-488 (2015).

11 Bendicho, S. l., Barbosa-Cánovas, G. V. & Martín, O. Milk processing by high intensity pulsed electric fields. *Trends in Food Science & Technology* **13**, 195-204 (2002).

12 Gusbeth, C., Frey, W., Volkmann, H., Schwartz, T. & Bluhm, H. Pulsed electric field treatment for bacteria reduction and its impact on hospital wastewater. *Chemosphere* **75**, 228-233 (2009).

13 Sengel, J. T. & Wallace, M. I. Imaging the dynamics of individual electropores. *Proceedings of the National Academy of Sciences* **113**, 5281-5286 (2016).
14 Kotnik, T., Rems, L., Tarek, M. & Miklavčič, D. Membrane electroporation and electropermeabilization: mechanisms and models. *Annual review of biophysics* **48**, 63-91 (2019).
15 Tieleman, D. P., Leontiadou, H., Mark, A. E. & Marrink, S.-J. Simulation of pore formation in lipid bilayers by mechanical stress and electric fields. *Journal of the American Chemical Society* **125**, 6382-6383 (2003).
16 Wang, T., Chen, H., Yu, C. & Xie, X. Rapid determination of the electroporation threshold for bacteria inactivation using a lab-on-a-chip platform. *Environment international* **132**, 105040 (2019).
17 Yildiz, S., Pokhrel, P. R., Unluturk, S. & Barbosa-Canovas, G. V. Shelf life extension of strawberry juice by equivalent ultrasound, high pressure, and pulsed electric fields processes. *Food Research International* **140**, doi:10.1016/j.foodres.2020.110040 (2021).
18 Rojas-Chapana, J. A., Correa-Duarte, M. A., Ren, Z., Kempa, K. & Giersig, M. Enhanced introduction of gold nanoparticles into vital acidothiobacillus ferrooxidans by carbon nanotube-based microwave electroporation. *Nano Letters* **4**, 985-988 (2004).
19 Liu, C. *et al.* Conducting nanosponge electroporation for affordable and high-efficiency disinfection of bacteria and viruses in water. *Nano letters* **13**, 4288-4293 (2013).
20 Zhou, J., Wang, T., Chen, W., Lin, B. & Xie, X. Emerging investigator series: locally enhanced electric field treatment (LEEFT) with nanowire-modified electrodes for water disinfection in pipes. *Environmental Science: Nano* (2020).
21 Zhou, J., Wang, T., Yu, C. & Xie, X. Locally enhanced electric field treatment (LEEFT) for water disinfection. (2020).
22 Zhou, J., Yu, C., Wang, T. & Xie, X. Development of Nanowire-Modified Electrodes Applied in the Locally Enhanced Electric Field Treatment (LEEFT) for Water Disinfection. *Journal of Materials Chemistry A* (2020).
23 Huo, Z.-Y. *et al.* Nanowire-modified three-dimensional electrode enabling low-voltage electroporation for water disinfection. *Environmental science & technology* **50**, 7641-7649 (2016).
24 Huo, Z.-Y. *et al.* Carbon-nanotube sponges enabling highly efficient and reliable cell inactivation by low-voltage electroporation. *Environmental Science: Nano* **4**, 2010-2017 (2017).
25 Huo, Z.-Y. *et al.* A Cu 3 P nanowire enabling high-efficiency, reliable, and energy-efficient low-voltage electroporation-inactivation of pathogens in water. *Journal of Materials Chemistry A* **6**, 18813-18820 (2018).
26 Huo, Z.-Y. *et al.* Low-voltage alternating current powered polydopamine-protected copper phosphide nanowire for electroporation-disinfection in water. *Journal of materials chemistry A* **7**, 7347-7354 (2019).
27 Zhou, J., Wang, T. & Xie, X. Locally Enhanced Electric Field Treatment (LEEFT) Promotes the Performance of Ozonation for Bacteria Inactivation by Disrupting the Cell Membrane. *Environmental Science & Technology* **54**, 14017-14025 (2020).

28 Lapizco-Encinas, B. H., Simmons, B. A., Cummings, E. B. & Fintschenko, Y. Dielectrophoretic concentration and separation of live and dead bacteria in an array of insulators. *Analytical chemistry* **76**, 1571-1579 (2004).
29 Zhou, J., Wang, T., Yu, C. & Xie, X. Locally enhanced electric field treatment (LEEFT) for water disinfection. *Frontiers of Environmental Science & Engineering* **14**, 1-12 (2020).
30 Zhang, T. *et al.* Inactivation of Bacteria by Peracetic Acid Combined with Ultraviolet Irradiation: Mechanism and Optimization. *Environmental Science & Technology* **54**, 9652-9661 (2020).
31 Huang, X. *et al.* Investigation of functional selenium nanoparticles as potent antimicrobial agents against superbugs. *Acta biomaterialia* **30**, 397-407 (2016).
32 Guo, Y. *et al.* Detection of reactive oxygen species (ROS) generated by TiO2 (R), TiO2 (R/A) and TiO2 (A) under ultrasonic and solar light irradiation and application in degradation of organic dyes. *Journal of hazardous materials* **192**, 786-793 (2011).
33 Vaessen, E., Timmermans, R., Tempelaars, M., Schutyser, M. & den Besten, H. Reversibility of membrane permeabilization upon pulsed electric field treatment in lactobacillus plantarum WCFS1. *Scientific reports* **9**, 1-11 (2019).
34 Liu, H. *et al.* Carbon fiber-based flow-through electrode system (FES) for water disinfection via direct oxidation mechanism with a sequential reduction–oxidation process. *Environmental science & technology* **53**, 3238-3249 (2019).
35 Boukany, P. E. *et al.* Nanochannel electroporation delivers precise amounts of biomolecules into living cells. *Nature nanotechnology* **6**, 747-754 (2011).
36 Mai-Prochnow, A., Clauson, M., Hong, J. & Murphy, A. B. Gram positive and Gram negative bacteria differ in their sensitivity to cold plasma. *Scientific reports* **6**, 1-11 (2016).